The Protein-Tyrosine Phosphatase Receptor Type J is regulated by the pVHL-HIF axis in Clear Cell Renal Cell Carcinoma

Casagrande, Silvia ; Ruf, Melanie ; Rechsteiner, Markus ; Morra, Laura ; Brun-Schmid, Sonja ; von Teichman, Adriana ; Krek, Wilhelm ; Schraml, Peter ; Moch, Holger

Abstract: Mass spectrometry analysis of renal cancer cell lines recently suggested that the Protein-Tyrosine Phosphatase Receptor Type J (PTPRJ), an important regulator of tyrosine kinase receptors, is tightly linked to the von-Hippel Lindau protein (pVHL). Therefore, we aimed to characterize the biological relevance of PTPRJ for clear cell renal cell carcinoma (ccRCC). In pVHL negative ccRCC cell lines both RNA and protein expression levels of PTPRJ were lower than those in the corresponding pVHL reconstituted cells. Quantitative RT-PCR and Western blot analysis of ccRCC with known VHL mutation status and normal matched tissues as well as RNA in situ hybridization on a Tissue Microarray (TMA) confirmed a decrease of PTPRJ expression in more than 80 % of ccRCCs, but in only 12 % of papillary RCCs. ccRCC patients with no or reduced PTPRJ mRNA expression had a less favourable outcome than those with a normal expression status ($p = 0.05$). Sequence analysis of 32 PTPRJ mRNA negative ccRCC samples showed five known polymorphisms, but no mutations implying other mechanisms leading to PTPRJ's down-regulation. Selective silencing of HIF- by siRNA and reporter gene assays demonstrated that pVHL inactivation reduces PTPRJ expression through a HIF-dependent mechanism, which is mainly driven by HIF-2 stabilization. Our results suggest PTPRJ as a member of a pVHL controlled pathway whose suppression by HIF is critical for ccRCC development. Copyright © 2012 Pathological Society of Great Britain and Ireland. Published by John Wiley Sons, Ltd.

DOI: https://doi.org/10.1002/path.4107

The Protein-Tyrosine Phosphatase Receptor Type J is regulated by the pVHL-HIF axis in Clear Cell Renal Cell Carcinoma

Running Title:

PTPRJ in Clear Cell Renal Cell Carcinoma

Silvia Casagrande[1], Melanie Ruf[1], Markus Rechsteiner[1], Laura Morra[1], Sonja Brun-Schmid[1], Adriana von Teichman[1], Wilhelm Krek[2], Peter Schraml[1]* and Holger Moch[1]*

[1]Institute of Surgical Pathology, University Hospital Zurich, Schmelzbergstrasse 12, 8091, Zurich, Switzerland.

[2] Institute of Molecular Health Sciences, Swiss Federal Institute of Technology (ETH) Zurich, 8093 Zurich, Switzerland.

* shared last co-authorship

Correspondence:

Peter Schraml, Ph.D.

Institute of Surgical Pathology, University Hospital Zurich, Schmelzbergstrasse 12, 8091, Zurich, Switzerland.

Tel.: +41 -44 255 2114; Fax: +41 -44 255 4440

Peter.Schraml@usz.ch

The authors declare no conflict of interest.

This article has been accepted for publication and undergone full peer review but has not been through the copyediting, typesetting, pagination and proofreading process, which may lead to differences between this version and the Version of Record. Please cite this article as doi: 10.1002/path.4107.

ABSTRACT

Mass spectrometry analysis of renal cancer cell lines recently suggested that the Protein-Tyrosine Phosphatase Receptor Type J (PTPRJ), an important regulator of tyrosine kinase receptors, is tightly linked to the von-Hippel Lindau protein (pVHL). Therefore, we aimed to characterize the biological relevance of PTPRJ for clear cell renal cell carcinoma (ccRCC). In pVHL negative ccRCC cell lines both RNA and protein expression levels of PTPRJ were lower than those in the corresponding pVHL reconstituted cells. Quantitative RT-PCR and Western blot analysis of ccRCC with known *VHL* mutation status and normal matched tissues as well as RNA *in situ* hybridization on a Tissue Microarray (TMA) confirmed a decrease of *PTPRJ* expression in more than 80 % of ccRCCs, but in only 12 % of papillary RCCs. ccRCC patients with no or reduced *PTPRJ* mRNA expression had a less favourable outcome than those with a normal expression status (p=0.05). Sequence analysis of 32 *PTPRJ* mRNA negative ccRCC samples showed five known polymorphisms, but no mutations implying other mechanisms leading to PTPRJ's down-regulation. Selective silencing of HIF-α by siRNA and reporter gene assays demonstrated that pVHL inactivation reduces *PTPRJ* expression through a HIF-dependent mechanism, which is mainly driven by HIF-2α stabilization. Our results suggest *PTPRJ* as a member of a pVHL controlled pathway whose suppression by HIF is critical for ccRCC development.

Key words:

RCC, VHL/HIF pathway, PTPRJ

INTRODUCTION

Most clear cell renal cell carcinomas (ccRCC) are characterized by a bi-allelic somatic inactivation of the von Hippel-Lindau (*VHL*) tumour suppressor gene [1]. The VHL protein (pVHL) is an important regulator of the Hypoxia Inducible Factor-α (HIF-α), microtubule stabilization, maintenance of the primary cilium, mitotic regulation and cell mobility [2]. The loss of function of pVHL leads to HIF-α stabilization and up-regulation of HIF target genes which are involved in cell growth and proliferation, angiogenesis, invasion and metastasis. Examples of up-regulated HIF-target genes are VEGF-A, EPO, EGFR and CAIX [3] which represent also potential anticancer drug targets. Data about genes and proteins down-regulated due to pVHL functional deficiency are rare. Examples include important genes/proteins such as fibronectin [4], E-cadherin [5], PAX2 [6] and p53 [7].

Recent mass spectrometry experiments with ccRCC cell lines [8] showed that the expression of the protein tyrosine phosphatase receptor type J (PTPRJ) is associated with the presence of pVHL. PTPRJ is composed of an extracellular domain that contains eight fibronectin type III repeats, a transmembrane domain, and a cytoplasmic end comprising a single catalytic domain [9]. *In vitro*, the receptor is involved in the regulation of cellular differentiation, proliferation, growth and migration [10-14] which supports its potential relevance for cancer development. In colon, lung and breast cancer *PTPRJ* is affected by allelic imbalances and missense mutations [15, 16]. Furthermore, several membrane-associated tyrosine kinase receptors are controlled by PTPRJ, among them there are established or potential molecular anti-cancer drug targets, e.g. EGFR [17], PDGFR-β [18], VEGFR2 [19] and HGFR (also termed c-MET) [20].

To date the molecular mechanisms leading to down-regulation of *PTPRJ* expression in ccRCC are unknown. Consequently, here we investigated the influence of the pVHL-HIF axis on *PTPRJ* expression in human ccRCC.

MATERIALS AND METHODS

Tissue specimens and tissue microarray

For quantitative RT-PCR analysis of *PTPRJ* mRNA levels, frozen tissue samples of 17 ccRCCs and matched non-tumorous tissue were used. The pathological parameters of the ccRCCs are presented together with the *VHL* mutations in Table S1 (supplementary data). A previously described tissue microarray (TMA) was used [21] to determine *PTPRJ* mRNA expression in ccRCCs, pRCC and normal kidney samples. This study was approved by the local commission of ethics (reference number StV. 38-2005). All tissue specimens were supplied by the tissue biobank of the University Hospital Zurich.

mRNA quantification

Quantitative analysis of *PTPRJ* mRNA expression was performed by qRT-PCR using 17 ccRCCs with known *VHL* mutation status. Normal matched tissue was available for each tumour and used as control. Total RNA was isolated using the RNeasy Mini Kit (Qiagen, Hilden, Germany) and quantified using the Nanodrop spectrometer. Total RNA (0.2 to 1 μg) was reverse-transcribed using the High Capacity cDNA Reverse Transcription Kit (Applied Biosystems, Foster City, CA, USA). The expression of the mRNAs of *PTPRJ*, *HIF-1α*, *HIF-2α*, and *GLUT-1* was quantified using the following TaqMan gene expression assays: Hs00174561_m1 (*PTPRJ*), Hs00936376_m1 (*HIF-1α*), Hs01026146_m1 (*HIF-2α*), and Hs00197884_m1 (*GLUT-1*). The expression assays were designed by Applied Biosystems and analysed using the 7900 Fast Real-time PCR System (Applied Biosystems). The data

were quantified with the comparative C_t method for relative gene expression and normalised using *PPIA* (expression assay Hs99999904_m1) [22].

RNA *in situ* hybridization (RISH)

PTPRJ mRNA expression was analysed on a TMA by non-radioactive *in situ* hybridisation adapted from a previously published protocol [23]. Briefly, total mRNA was extracted from HeLa cells and the following primers containing the T7 polymerase binding site (5'-TAATACGACTCACTATAGGGAGAG-3') were chosen to amplify two parts of the *PTPRJ* mRNA: 5'-GTGAAAGCTCTGGAGCCAAC-3' and 5'-ACTCCTCATGGCTTCCAATG-3' spanning exons 3-5 and 5'- GAGATCGGCTTAGCATGGAG-3' and 5'-TATAAGGTGCCCGGAATCAG-3' spanning exons 8-9. Digoxigenin (DIG)-labelled antisense and sense riboprobes were transcribed *in vitro* with T7 RNA polymerase in the presence of digoxigenin-UTP (Roche Applied Science). For the hybridization procedure 1-2 µl of DIG-labelled sense and antisense probes (about 100-200 ng) were added to the hybridization mix and denatured at 85°C for 5 min. Two µm thick TMA sections were incubated at 60°C overnight. Detection of probe-target hybrids was performed with NBT/BCIP substrate (Roche Applied Science). The intensity of the staining for *PTPRJ* mRNA expression was classified as follows: 0 negative staining, +1 reduced staining, +2 strong staining. The intensity of staining detected in normal proximal tubules was considered as reference for strong staining.

Mutation analysis of *PTPRJ* and *VHL*

For the mutation analysis of *PTPRJ* genomic DNA was extracted from 32 formalin fixed and paraffin embedded ccRCCs which were also on the large TMA. Five normal matched tissues were included in the analysis. The mutation analysis of *PTPRJ* and *VHL* was performed as

previously described [16, 24]. Mutations were confirmed with at least one separate PCR and sequence analysis.

Cell lines

The ccRCC cell lines 786-O and RCC4 (transfected with empty vector), 786-O VHL (stably expressing pVHL), RCC4 Y98H and RCC4 Y98N (stably expressing the Type 2A and the Type 2B pVHL mutants Y98H and Y98N, respectively) were used in this study. All cell lines were grown under conditions recommended by ATCC and authenticated by short tandem repeat profiling by Identicell (Department of Molecular Medicine, Aarhus University, Hospital Skejby, Aarhus, Denmark).

Western blotting and antibodies

Total cell lysates were prepared with RIPA buffer (Sigma-Aldrich Corp, Saint Louis, MO, USA) supplemented with protease inhibitors (Complete protease inhibitor cocktail, Roche, Basel, Switzerland). For cell and tissue fractioning a Nuclear Extraction Kit (Active Motif, Carlsbad, CA, USA) and the TissueLyser (Qiagen, Hilden, Germany) were used, respectively. Western blot was done as described [6]. Primary antibodies used were anti-pVHL (diluted 1:500; provided by Wilhelm Krek, ETH Zurich), anti-HIF-1α (1:1000; Cell Signalling, Danvers, MA, USA), anti-HIF-2α (1:200; NB 100-122, Novus Biologicals, Littleton, CO, USA), anti-β-actin (1:1000; Chemicon International, Temecula, CA, USA); anti-PTPRJ (cell line extracts) (1:200; H300 sc-22749, Santa Cruz Biotechnology, Santa Cruz, CA, USA) and anti-PTPRJ (cell line and tissue extracts) (1:500; Proteintech, Chicago, IL, USA). Secondary antibodies were HRP-conjugated anti-mouse (1:2000; ab672, Abcam) and HRP-conjugated anti-rabbit (1:2000; Millipore, Billerica, MA, USA). The protein-antibody complexes were detected by using ECL (Amersham, Little Chalfont, Buckinghamshire HP7 7NA United

Kingdom). Band intensities of PTPRJ and β-Actin from Western blots were measured using ImageJ software.

Transient transfections

For RNA interference experiments RCC4, 786-O and HK2 cells were transfected with 5 nM siRNA oligonucleotides using HiPerfect transfection reagent (Qiagen). The siRNA sequences (Qiagen; Life Technologies, Carlsbad, CA, USA) are listed in Table S2 (supplementary data). AllStars Negative controls (Qiagen) was used as negative control. To study the effects of PTPRJ overexpression in RCC4 cells, the pQE-TriSystem-6 vector (Qiagen) containing the ORF of the *PTPRJ* gene (Entrez Gene: 5795, Ensembl: ENSG00000149177, UniProtKB: Q12913) was used. The pQE-TriSystem-6 served as control (empty vector). Cells were grown for 24 h in a 6-well format and then transiently transfected with the expression vector. Cells were harvested after 96 h to evaluate PTPRJ expression levels by qRT-PCR and Western blot.

Luciferase gene reporter assay

Luciferase gene expression assays were performed as previously described [6]. The nucleotides between -2682 and +515 were defined as the putative promoter region of *PTPRJ* (Chr. 11p11.2; 47,971,665:48,222,839, positive strand, NCBI) considering the A(TG) translation site as +1 reference. The promoter region was synthesized from GenScript (Piscataway, NJ, USA) and cloned into firefly luciferase reporter plasmid pGL4.10 (Promega, Madison, WI, USA). pGL4.10P2P vector containing wild type *P2P* hypoxia response elements (HREs) of the human *PHD2* promoter were provided by Roland Wenger (University of Zurich, Switzerland) and was used as positive control as previously described [6, 25].

For transcriptional transactivation experiments, 786-O cells were transfected with siRNA (HIF-2α #1 or siScr) and grown in a 24-well format. After 48 h the cells were transfected with 1 μg luciferase reporter plasmid and 200 ng pGL4.74 renilla luciferase reporter plasmid (Promega) using FuGene 6 reagent (Roche Molecular Biochemicals). Luciferase activity was measured 24 h later after cell lysis using the Dual-Luciferase reporter assay system (Promega). Relative luciferase units were determined according to the manufacturer's instructions (Promega) to generate the ratio of the values obtained from siHIF-2α and siSc treatments.

MTT proliferation assay

RCC4 cells were grown in a 6-well format for 24 h and transfected with the expression or control vector. MTT proliferation assay (Cell Proliferation Kit I MTT, Roche) was performed according to the manufacturer's protocol. Briefly, transfected cells were plated in a 96-well plate. After the incubation period, 10 μl of the MTT labelling reagent (final concentration 0.5 mg/ml) was added to each well and cells were incubated for 4 h. Subsequently, 100 μl of the solubilisation solution was added to the wells and cells were incubated overnight at 37°C. The solubilized formazan product was quantified using an ELISA reader (Tecan, Infinite f200) at wavelength 570 nm. The analysis of cell proliferation was performed after 96 h, 120 h, 144 h and 168 h.

Statistical analysis

Analysis between groups was done with 2-way ANOVA and post-hoc Bonferroni multiple comparison (GraphPad Prism 5). Contingency table analysis and Pearson's Chi-squared tests were calculated using SPSS 17.0 statistical software package. Survival curves were estimated with the Kaplan–Meier method and the log rank test. P values ≤ 0.05 were considered statistically significant.

RESULTS

Direct correlation of PTPRJ and pVHL expression in RCC cell lines

Previous mass spectrometry experiments performed with pVHL-deficient and pVHL-re-expressing RCC cell lines identified PTPRJ positively linked to pVHL expression [8]. To confirm that *PTPRJ* is influenced by the VHL/HIF axis we used the pVHL-deficient renal cancer cell lines 786-O and RCC4 and their corresponding stable pVHL transfectants. Compared to the correspondent pVHL-negative cell lines both *PTPRJ* mRNA (Fig. 1A) and protein levels (Fig. 1B and 1C) were increased in the presence of pVHL.

PTPRJ mRNA expression is decreased in ccRCC tissue

To quantitatively evaluate *PTPRJ* mRNA expression in human RCC samples we performed qRT-PCR with 17 ccRCCs and normal matched tissues. *PTPRJ* expression was reduced in 15 of 17 ccRCCs (88 %) (Fig. 1D) when compared to normal renal tissues. A strong *PTPRJ* expression was seen in one *VHL* wild type tumour and in one ccRCC with a missense mutation that causes an amino acid exchange at codon 88 (Fig. 1D, Table S1). Western blot analysis with three matched normal/tumour pairs demonstrated a direct correlation between mRNA and protein expression of PTPRJ (Fig. 1E).

As commercially available PTPRJ antibodies were not specific in formalin fixed and paraffin embedded tissues, the expression of *PTPRJ* was analysed by RNA *in situ* hybridization (RISH). The specificity of DIG-labelled RNA probes for *PTPRJ* was confirmed by Northern Blot analysis using total RNA from HeLa cells (positive control). The antisense probes bound a 7.8 kb band corresponding to the *PTPRJ* transcript (data not shown).

PTPRJ RISH analysis on a TMA showed strong positivity in the proximal tubular cells of all analysed normal kidney tissue samples (Fig. 2), whereas in 198 of 232 (85 %) analysable ccRCCs, but in only 5 of 41 (12 %) of pRCCs *PTPRJ* expression was reduced ($p < 0.001$). ccRCC patients with no or low *PTPRJ* mRNA expression showed a worse prognosis than those with a normal expression status ($p=0.05$) (Fig. 3). No associations were seen between *PTPRJ* expression and tumour stage and grade. The highly significant difference between the survival curves of patients with organ-confined and locally advanced tumours confirmed the validity of the clinical data (Fig S2).

Mutation analysis of *PTPRJ* in ccRCC

Twenty-two *PTPRJ* negative and 10 weakly expressing ccRCC samples included in the TMA were selected for mutation analysis of exons 5, 6, 7 and 13 of *PTPRJ*. So far, all cancer-related amino-acid substitutions were identified in these four exons which code the extracellular portion responsible for interactions with ligands or other proteins [16]. Five normal matched tissues were also included in this analysis. We found two conservative (E206E and T233T) and three non-conservative (Q276P, R326Q and E872D) polymorphisms which were previously reported (UniprotKB/Swiss-Prot, Q12913 (PTPRJ_HUMAN)). There were no mutations affecting the reading frame of *PTPRJ*.

PTPRJ expression is HIF-2α-dependent

To determine the influence of the pVHL-HIF axis on *PTPRJ* expression we used different pVHL expressing and non-expressing RCC cell lines. In RCC4 cells expressing the pVHL mutant Y98N, which fail to degrade HIF-α [26], *PTPRJ* mRNA expression was comparable to pVHL-deficient RCC4. In contrast, RCC4 cells expressing the pVHL mutant Y98H, which has only a slight defect in ubiquitination of HIF-α [26], the *PTPRJ* mRNA level

was increased and similar to the RCC4 VHL cell line (Fig. 4A). An opposite effect was observed with *GLUT1* mRNA whose expression increased in the presence of HIF-α (Fig. 4B).

Next, we silenced HIF-1α and HIF-2α by siRNA in the pVHL-deficient RCC4 cell line to determine whether the two HIF-α isoforms were able to down-regulate *PTPRJ* mRNA expression. Efficient knock down of HIF-1α and HIF-2α was confirmed by qRT-PCR and Western blot analysis (Fig. 4C-G). In RCC4, silencing of HIF-1α had positive effects on *PTPRJ* mRNA expression after 48 h (Fig. 5A). In contrast, silencing of HIF-2α produced an increase of *PTPRJ* mRNA expression already after 24 h and reached a 2-fold up-regulation after 48 h (Fig. 5B). We also silenced HIF-2α by siRNA in the pVHL and HIF-1α -null 786-O cell line. After 48 h we obtained an increase of *PTPRJ* mRNA expression which was comparable to that observed in 786-O VHL (Fig. 5D). Efficient knock down of HIF-2α was confirmed by analysing the level of *GLUT-1* mRNA (Fig. 5F). Western blot analysis confirmed a strong increase of PTPRJ protein expression in both HIF-2α silenced ccRCC cell lines (Fig. 5C and E). Similar results were obtained with two additional HIF-2α siRNAs excluding possible off target effects (Fig. S1 A-C).

HIF response elements in the promoter region influence *PTPRJ* expression

The putative promoter region of *PTPRJ* contains five HREs and three reverse HREs (Table S3, Fig. 6A). To study the influence of the HREs on *PTPRJ* expression a luciferase reporter plasmid pGL4.10 construct containing 3.2kb of the *PTPRJ* promoter was generated (Fig. 6A). By silencing HIF-2α in 786-O cells (Fig. 6B) the reporter activity of the vector increased significantly compared to those of the empty plasmid and the *P2P* promoter construct (Fig. 6C). These results show that HIF-2α negatively regulates *PTPRJ* via the identified putative HREs in its promoter region.

PTPRJ regulates cell proliferation

RCC4 cells transfected with Qiagen expression vector pQE-TriSystem 6 containing the *PTPRJ* gene showed increased mRNA and protein expression of PTPRJ (Fig. 6D and 6E). RCC4 cells transfected with the *PTPRJ* vector showed a significant reduced proliferation rate compared to the control group (Fig. 6F).

We also silenced *PTPRJ* by siRNA in wild type pVHL expressing HK2 to see if PTPRJ down regulation leads to increased cell proliferation in the presence of pVHL. Reduced expression negatively influenced cell proliferation after 72 h (Fig. S3A-B) and suggests that loss of PTPRJ is biologically relevant to promote growth of ccRCC, independently from the pVHL expression status.

DISCUSSION

We have demonstrated that decreased *PTPRJ* expression is characteristic for the vast majority of ccRCC. *In vitro* experiments showed that higher *PTPRJ* mRNA and protein expression levels are closely linked to the presence of functional pVHL. Down-regulation of *PTPRJ* is mainly dependent on HIF-2α stabilisation following pVHL loss.

Our TMA analysis showed no or low *PTPRJ* mRNA expression in 85 % of ccRCCs, whereas in most of the pRCCs *PTPRJ* mRNA levels were comparable to those in normal tissues. The fact that *VHL* is mutationally affected in about 70-80 % of ccRCCs [1, 27, 28], suggests a close relationship between *PTPRJ* mRNA expression and pVHL functional integrity. This is supported by the observation that *PTPRJ* expression was normal in almost 90 % of the analysed pRCC in which *VHL* is hardly mutated [29]. This result confirms our recent proteomics finding of a relationship between *PTPRJ* expression and pVHL in human tissue [8]. In our test set of 17 ccRCC reduced *PTPRJ* mRNA expression was also seen in two

of four tumours with wild type *VHL*. Other mechanisms of *VHL* inactivation, such as tumour hypoxia or hypermethylation of the *VHL* promoter, which occurs in about half of *VHL* wild type ccRCC [1, 28, 30], may explain this observation.

Here, we identified *PTPRJ* as potential target of HIF-2α. HIF-1α and HIF-2α share high similarity in their DNA binding and dimerization domains, but they differ in their transactivation domains [31]. As a consequence, there are common gene targets, but also genes that are preferentially regulated by one of the two isoforms. HIF-1α seems to preferentially drive the transcription of genes encoding glycolytic enzymes and pro-apoptotic factors, such as BCL2/adenovirus E1B–interacting protein 1, NIP3 (BNIP3). In contrast, HIF-2α induces the expression of pro-survival factors such as VEGF, TGF-α, and CCND1 [32]. Studies demonstrated that HIF-α can also down-regulate genes either by inducing repressors of transcription and by directly binding to hypoxia response elements (HREs) or to reverse HREs. The latter are present in the antisense strand of the promoter of HIF target genes. Examples of genes directly down-regulated by HIF-1α are α-fetoprotein [33], PPAR-α [34] and RECK [35], whereas genes directly or indirectly down-regulated by HIF-2α have not been described to date.

The analysis of the putative *PTPRJ* promoter showed the presence of five putative HREs and three putative reverse HREs. Since we observed *PTPRJ* down-regulation in the presence of HIF-2α, we asked whether HIF could directly act as suppressor of *PTPRJ* transcription. Using 786-O cells, significant effects were seen with our luciferase gene reporter assays suggesting that the HREs and reverse HREs identified in the putative *PTPRJ* promoter region are important for suppressing *PTPRJ* expression by HIF-2α. It is of note that only a two-fold overexpression of *PTPRJ* in RCC4 cells was sufficient to produce a significant inhibitory effect on cell proliferation. Our result expands the findings of previous

studies that describe anti-proliferative properties of *PTPRJ* in non-RCC tumour cell lines [10, 12, 14].

To evaluate the presence of mutations of the *PTPRJ* gene, we performed a sequence analysis of the exons 5, 6, 7 and 13 of *PTPRJ* in 32 ccRCCs. We found two conservative and three non-conservative polymorphisms, but no mutation predicting severe consequences on PTPRJ function. Similar frequencies of these polymorphisms were found in studies which analysed the *PTPRJ* genotype in other tumour types and in other populations [36-38]. The real influence of these polymorphisms on *PTPRJ* expression and function is still not fully understood. Our results suggest that in ccRCC the down-regulation of *PTPRJ* expression is obviously not caused by mutations but mainly due to the deregulation of the pVHL/HIF pathway (Fig. 7).

PTPRJ's inhibitory effect on cell proliferation in ccRCC, as shown by us, and in other tumour types [14, 39 , 40] as well as its ability to regulate EGFR phosphorylation [17] suggest its important influence on the activity of EGFR. Although EGFR over-expression occurs in the majority of ccRCC and is correlated with rapid tumour cell proliferation and worse patient outcome [41, 42], anti-EGFR targeted therapies have shown only low response rates [43, 44]. As demonstrated in non-small cell lung cancer, the success of such therapies is obviously dependent on EGFR activating mutations [45] which have not been found in ccRCC [41]. Antibodies against phosphorylated and activated EGFR are available but their use for reliably determining its tyrosine kinase activity status on formalin fixed, paraffin embedded tissue in routine diagnostics is challenging [46]. Despite the low number of tumors analysed, our Western blot data indicate reduced PTPRJ expression also at the protein level in a subset of ccRCC. It is conceivable that EGFR positive tumours with strongly reduced PTPRJ may better respond to inhibitors against EGFR and its downstream targets, such as

PI3K, AKT and mTOR, than those showing normal PTPRJ expression. However, additional experiments using optimized antibodies as well as appropriate mouse models are needed to characterize the biological relevance of PTPRJ down regulation by the pVHL/HIF axis and its clinical applicability for this tumour subtype.

In summary, we show that down-regulation of *PTPRJ* is a characteristic feature in ccRCC that is closely linked to the loss of pVHL function and the activation of HIF. Molecular studies of low abundant genes, such as *PTPRJ,* are a big challenge in cancer research as they are more sophisticated compared to investigations of those genes that become clearly up or down-regulated in tumours. They are nevertheless necessary to better understand the complex genetic network of cancer.

ACKNOWLEDGEMENTS

We thank Roger Santimaria and Martina Storz for the excellent technical assistance.

We thank Daniel Stiehl and Claudio Thoma for the luciferase vectors and cell lines, respectively. The study was supported by the Swiss National Science Foundation to H.M. (3238BO-103145) and the Zurich Cancer League to H.M.

STATEMENT OF AUTHOR CONTRIBUTIONS

S.C. and M.Ru. conceived and carried out experiments and generated the figures, M.Re. conceived experiments and interpreted data, L.M., S.B.-S. and A.v.T. carried out experiments, W.K. designed the study, P.S. and H.M. designed the study, analysed data and wrote the manuscript. H.M. reviewed the tumors. All authors had final approval of the submitted and published versions.

REFERENCES

1. Banks RE, Tirukonda P, Taylor C *et al.* Genetic and epigenetic analysis of von Hippel-Lindau (VHL) gene alterations and relationship with clinical variables in sporadic renal cancer. *Cancer Res* 2006; **66**: 2000-2011.
2. Frew IJ, Krek W. Multitasking by pVHL in tumour suppression. *Curr Opin Cell Biol* 2007; **19**: 685-690.
3. Gossage L, Eisen T. Alterations in VHL as potential biomarkers in renal-cell carcinoma. *Nat Rev Clin Oncol* 2010; **7**: 277-288.
4. Bluyssen HA, Lolkema MP, van Beest M *et al.* Fibronectin is a hypoxia-independent target of the tumor suppressor VHL. *FEBS Lett* 2004; **556**: 137-142.
5. Esteban MA, Tran MG, Harten SK *et al.* Regulation of E-cadherin expression by VHL and hypoxia-inducible factor. *Cancer Res* 2006; **66**: 3567-3575.
6. Luu VD, Boysen G, Struckmann K *et al.* Loss of VHL and hypoxia provokes PAX2 up-regulation in clear cell renal cell carcinoma. *Clin Cancer Res* 2009; **15**: 3297-3304.
7. Roe JS, Kim H, Lee SM *et al*. p53 stabilization and transactivation by a von Hippel-Lindau protein. *Mol Cell* 2006; **22**: 395-405.
8. Boysen G, Bausch-Fluck D, Thoma CR *et al.* Identification and Functional Characterization of pVHL-Dependent Cell Surface Proteins in Renal Cell Carcinoma. *Neoplasia* 2012; **14**: 535-546.
9. Honda H, Inazawa J, Nishida J *et al*. Molecular cloning, characterization, and chromosomal localization of a novel protein-tyrosine phosphatase, HPTP eta. *Blood* 1994; **84**: 4186-4194.
10. Balavenkatraman KK, Jandt E, Friedrich K *et al.* DEP-1 protein tyrosine phosphatase inhibits proliferation and migration of colon carcinoma cells and is upregulated by protective nutrients. *Oncogene* 2006; **25**: 6319-6324.

11. Jandt E, Denner K, Kovalenko M *et al*. The protein-tyrosine phosphatase DEP-1 modulates growth factor-stimulated cell migration and cell-matrix adhesion. *Oncogene* 2003; **22**: 4175-4185.

12. Kellie S, Craggs G, Bird IN *et al*. The tyrosine phosphatase DEP-1 induces cytoskeletal rearrangements, aberrant cell-substratum interactions and a reduction in cell proliferation. *J Cell Sci* 2004; **117**: 609-618.

13. Trapasso F, Iuliano R, Boccia A *et al.* Rat protein tyrosine phosphatase eta suppresses the neoplastic phenotype of retrovirally transformed thyroid cells through the stabilization of p27(Kip1). *Mol Cell Biol* 2000; **20**: 9236-9246.

14. Trapasso F, Yendamuri S, Dumon KR *et al.* Restoration of receptor-type protein tyrosine phosphatase eta function inhibits human pancreatic carcinoma cell growth in vitro and in vivo. *Carcinogenesis* 2004; **25**: 2107-2114.

15. Ruivenkamp C, Hermsen M, Postma C *et al.* LOH of PTPRJ occurs early in colorectal cancer and is associated with chromosomal loss of 18q12-21. *Oncogene* 2003; **22**: 3472-3474.

16. Ruivenkamp CA, van Wezel T, Zanon C *et al.* Ptprj is a candidate for the mouse colon-cancer susceptibility locus Scc1 and is frequently deleted in human cancers. *Nat Genet* 2002; **31**: 295-300.

17. Tarcic G, Boguslavsky SK, Wakim J *et al.* An unbiased screen identifies DEP-1 tumor suppressor as a phosphatase controlling EGFR endocytosis. *Curr Biol* 2009; **19**: 1788-1798.

18. Kovalenko M, Denner K, Sandstrom J *et al.* Site-selective dephosphorylation of the platelet-derived growth factor beta-receptor by the receptor-like protein-tyrosine phosphatase DEP-1. *J Biol Chem* 2000; **275**: 16219-16226.

19. Grazia Lampugnani M, Zanetti A, Corada M *et al.* Contact inhibition of VEGF-induced proliferation requires vascular endothelial cadherin, beta-catenin, and the phosphatase DEP-1/CD148. *J Cell Biol* 2003; **161**: 793-804.

20. Palka HL, Park M, Tonks NK. Hepatocyte growth factor receptor tyrosine kinase met is a substrate of the receptor protein-tyrosine phosphatase DEP-1. *J Biol Chem* 2003; **278**: 5728-5735.

21. Mertz KD, Demichelis F, Kim R *et al.* Automated immunofluorescence analysis defines microvessel area as a prognostic parameter in clear cell renal cell cancer. *Hum Pathol* 2007; **38**: 1454-1462.

22. Jung M, Ramankulov A, Roigas J *et al.* In search of suitable reference genes for gene expression studies of human renal cell carcinoma by real-time PCR. *BMC Mol Biol* 2007; **8**: 47.

23. Theurillat JP, Zurrer-Hardi U, Varga Z *et al.* Distinct expression patterns of the immunogenic differentiation antigen NY-BR-1 in normal breast, testis and their malignant counterparts. *Int J Cancer* 2008; **122**: 1585-1591.

24. Schraml P, Frew IJ, Thoma CR *et al.* Sporadic clear cell renal cell carcinoma but not the papillary type is characterized by severely reduced frequency of primary cilia. *Mod Pathol* 2009; **22**: 31-36.

25. Metzen E, Stiehl DP, Doege K *et al*. Regulation of the prolyl hydroxylase domain protein 2 (phd2/egln-1) gene: identification of a functional hypoxia-responsive element. *Biochem J* 2005; **387**: 711-717.

26. Thoma CR, Frew IJ, Hoerner CR *et al*. pVHL and GSK3beta are components of a primary cilium-maintenance signalling network. *Nat Cell Biol* 2007; **9**: 588-595.

27. Rechsteiner MP, von Teichman A, Nowicka A *et al*. VHL gene mutations and their effects on hypoxia inducible factor HIFalpha: identification of potential driver and passenger mutations. *Cancer Res* 2011; **71**: 5500-5511.

28. Nickerson ML, Jaeger E, Shi Y *et al.* Improved identification of von Hippel-Lindau gene alterations in clear cell renal tumors. *Clin Cancer Res* 2008; **14**: 4726-4734.

29. Brauch H, Weirich G, Brieger J *et al.* VHL alterations in human clear cell renal cell carcinoma: association with advanced tumor stage and a novel hot spot mutation. *Cancer Res* 2000; **60**: 1942-1948.

30. Herman JG, Latif F, Weng Y *et al.* Silencing of the VHL tumor-suppressor gene by DNA methylation in renal carcinoma. *Proc Natl Acad Sci U S A* 1994; **91**: 9700-9704.

31. Hu CJ, Wang LY, Chodosh LA *et al*. Differential roles of hypoxia-inducible factor 1alpha (HIF-1alpha) and HIF-2alpha in hypoxic gene regulation. *Mol Cell Biol* 2003; **23**: 9361-9374.

32. Raval RR, Lau KW, Tran MG *et al.* Contrasting properties of hypoxia-inducible factor 1 (HIF-1) and HIF-2 in von Hippel-Lindau-associated renal cell carcinoma. *Mol Cell Biol* 2005; **25**: 5675-5686.

33. Mazure NM, Chauvet C, Bois-Joyeux B *et al*. Repression of alpha-fetoprotein gene expression under hypoxic conditions in human hepatoma cells: characterization of a negative hypoxia response element that mediates opposite effects of hypoxia inducible factor-1 and c-Myc. *Cancer Res* 2002; **62**: 1158-1165.

34. Narravula S, Colgan SP. Hypoxia-inducible factor 1-mediated inhibition of peroxisome proliferator-activated receptor alpha expression during hypoxia. *J Immunol* 2001; **166**: 7543-7548.

35. Lee KJ, Lee KY, Lee YM. Downregulation of a tumor suppressor RECK by hypoxia through recruitment of HDAC1 and HIF-1alpha to reverse HRE site in the promoter. *Biochim Biophys Acta* 2010; **1803**: 608-616.

36. Iuliano R, Le Pera I, Cristofaro C *et al.* The tyrosine phosphatase PTPRJ/DEP-1 genotype affects thyroid carcinogenesis. *Oncogene* 2004; **23**: 8432-8438.

37. Iuliano R, Palmieri D, He H *et al.* Role of PTPRJ genotype in papillary thyroid carcinoma risk. *Endocr Relat Cancer* 2010; **17**: 1001-1006.

38. Mita Y, Yasuda Y, Sakai A *et al.* Missense polymorphisms of PTPRJ and PTPN13 genes affect susceptibility to a variety of human cancers. *J Cancer Res Clin Oncol* 2010; **136**: 249-259.

39. Iuliano R, Trapasso F, Le Pera I *et al.* An adenovirus carrying the rat protein tyrosine phosphatase eta suppresses the growth of human thyroid carcinoma cell lines in vitro and in vivo. *Cancer Res* 2003; **63**: 882-886.

40. Keane MM, Lowrey GA, Ettenberg SA *et al*. The protein tyrosine phosphatase DEP-1 is induced during differentiation and inhibits growth of breast cancer cells. *Cancer Res* 1996; **56**: 4236-4243.

41. Minner S, Rump D, Tennstedt P *et al.* Epidermal growth factor receptor protein expression and genomic alterations in renal cell carcinoma. *Cancer* 2012; **118**: 1268-1275.

42. Moch H, Sauter G, Buchholz N *et al.* Epidermal growth factor receptor expression is associated with rapid tumor cell proliferation in renal cell carcinoma. *Hum Pathol* 1997; **28**: 1255-1259.

43. Drucker B, Bacik J, Ginsberg M *et al.* Phase II trial of ZD1839 (IRESSA) in patients with advanced renal cell carcinoma. *Invest New Drugs* 2003; **21**: 341-345.

44. Rowinsky EK, Schwartz GH, Gollob JA *et al.* Safety, pharmacokinetics, and activity of ABX-EGF, a fully human anti-epidermal growth factor receptor monoclonal antibody in patients with metastatic renal cell cancer. *J Clin Oncol* 2004; **22**: 3003-3015.

45. Lynch TJ, Bell DW, Sordella R *et al.* Activating mutations in the epidermal growth factor receptor underlying responsiveness of non-small-cell lung cancer to gefitinib. *N Engl J Med* 2004; **350**: 2129-2139.

46. Becker KF, Mack H, Schott C *et al.* Extraction of Phosphorylated Proteins from Formalin-Fixed Cancer Cells and Tissues. *Open Pathol Journal* 2008; **2**: 46-52.

FIGURE LEGENDS

Figure 1. Positive correlation between PTPRJ and pVHL expression. A) *PTPRJ* mRNA levels measured by qRT-PCR (3 replicas ± SD) in pVHL-negative RCC cell lines and their stable *VHL* transfectants (increase 1.5 to 1.9-fold). B) Western blot showing PTPRJ protein expression in VHL-negative ccRCC cells and their stable *VHL* transfectants (loading control: β-Actin). C) Elevated PTPRJ expression in pVHL expressing 786-O (normalized mean 1.73 $\pm$ 0.42 SD, n = 5, p = 0.026) and RCC4 cells (1.51 $\pm$ 0.64, n = 4, p = ns.). D) Normalized *PTPRJ* mRNA levels measured by qRT-PCR in 17 ccRCCs and their normal matched tissues (3 replicas ± SD). The *VHL* mutation status in the tumours is indicated (wt = wild type, ms = missense, del fs = deletion leading to frameshift, del ins = deletion and insertion, delX = deletion leading to a stop codon). E) Western blot showing PTPRJ protein expression in three ccRCC tissues and matched normal tissues (loading control: β-actin). Significant differences ($p < 0.05$) are indicated by asterisks.

Figure 2. *PTPRJ* RISH on a TMA with examples for negative, reduced and strong *PTPRJ* mRNA expression in ccRCC and normal kidney.

Figure 3. Kaplan-Meier plot of overall survival of ccRCC patients defined by *PTPRJ* mRNA expression. Survival data were not available from 18 patients. *PTPRJ* expression was defined reduced if the mRNA staining in a tumor was unequivocally weaker compared to that seen in normal kidney.

Figure 4. A) *PTPRJ* mRNA transcription in RCC4 VHL, RCC4 Y98H (HIF-α destabilising VHL mutation) and RCC4 Y98N (HIF-α non-destabilising VHL mutation) cells. B) *GLUT-1* mRNA expression in the same RCC4 cells. C and D) Knock down efficiency of siHIF-1α and siHIF-2α on *HIF-1α* (C) and *HIF-2α* (D) mRNA expression after 24 h and 48 h in RCC4 cells. E) Western blot showing down-regulated HIF-1α and HIF-2α protein expression in RCC4 cells. F) *HIF-2α* mRNA expression in siHIF-2α transfected 786-O cells after 24 h and 48 h. G) Western blot showing down-regulated HIF-2α protein expression (loading control: β-actin). Significant differences ($p < 0.05$) of *PTPRJ, GLUT-1, HIF-1α* and *HIF-2α* expression compared to wild type cell lines are indicated by asterisks.

Figure 5. PTPRJ expression depends mainly on HIF-2α. A) Increase of *PTPRJ* mRNA expression in RCC4 cells after silencing of HIF-1α and B) after silencing of HIF-2α. C) Western blot showing PTPRJ protein expression in RCC4 cells after silencing of HIF-1α and HIF-2α. D) Increase of *PTPRJ* mRNA levels in 786-O cells after silencing of HIF-2α. E) PTPRJ protein expression after silencing of HIF-2α. F) *GLUT-1* mRNA expression in HIF-2α silenced 786-O cells. Data represent mean of two experiments done in triplicate ± SD. Significant differences ($p < 0.05$) of *PTPRJ* and *GLUT-1* expression compared to wild type cell lines are indicated by asterisks.

Figure 6. *PTPRJ* promoter activity is HIF-2α dependent. A) Schematic representation of the 3.2 kb *PTPRJ* promoter with the location of the five HREs and three reverse HREs. B) Western blot showing efficient knock down of HIF-2α in 786-O cells after 72 h (loading control: β-actin). C) Luciferase reporter gene assay with *P2P* (HIF target) and *PTPRJ* vector constructs after transient transfection of siScrambled and siHIF-2α using 786-O cells. Decrease of *P2P* and increase of *PTPRJ* promoter activity after HIF-2α silencing. D) *PTPRJ* mRNA levels measured by qRT-PCR in RCC4 cells untreated, transfected with scrambled control and with *PTPRJ* expression vector 96 h after transfection. Data represent mean of 3 replicas ± SD. E) Immunoblot of PTPRJ expression in RCC4 cells untreated, transfected with scrambled control and with *PTPRJ* expression vector 96 h after transfection. RQ = relative quantification. F) Proliferation of RCC4 cells 96 h, 120 h, 144 h and 168 h after transfection with empty vector (control) or *PTPRJ* expression vector (PTPRJ).

Figure 7. Schematic representation of the HIF-α dependent regulation of *PTPRJ* expression in normal kidney and ccRCC.

SUPPLEMENTARY DATA

Figure S1. A) Western blot showing HIF-2α down regulation in 786-O cells with three different siHIF-2α (siHIF-2α #1, siHIF-2α #2, siHIF-2α #3) to exclude off target effects for changed PTPRJ expression. B) Increased *PTPRJ* mRNA levels in 786-O cells and C) in RCC4 cells after silencing of HIF-2α with siHIF-2α #2.

Figure S2. Kaplan-Meier plot of overall survival of ccRCC patients with organ-confined (stage pT1/pT2) and locally advanced tumors (pT3/pT4).

Figure S3. A) Western blot showing PTPRJ down regulation in HK2 cells 72 h after transfection. B) Proliferation of HK2 cells 24 h, 48 h, 72 h and 96 h after transfection of siPTPRJ and siScramled (control).

Figure 1

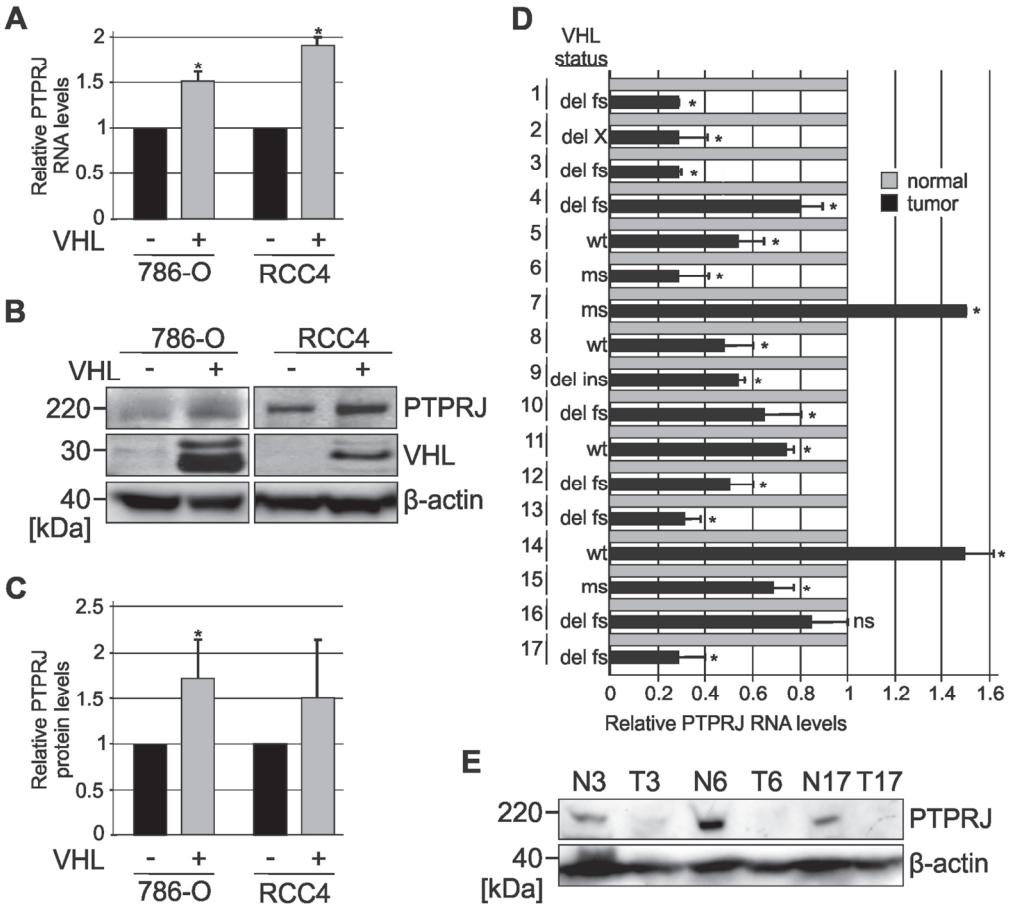
A
Relative PTPRJ RNA levels
2
1.5
1
0.5
0
VHL - + - +
786-O
RCC4
B
786-O
RCC4
VHL - + - +
220
30
40
[kDa]
PTPRJ
VHL
β-actin
C
Relative PTPRJ protein levels
2.5
2
1.5
1
0.5
0
VHL - + - +
786-O
RCC4
D
VHL status
1 del fs
2 del X
3 del fs
4 del fs
5 wt
6 ms
7 ms
8 wt
9 del ins
10 del fs
11 wt
12 del fs
13 del fs
14 wt
15 ms
16 del fs
17 del fs
normal
tumor
ns
0 0.2 0.4 0.6 0.8 1 1.2 1.4 1.6
Relative PTPRJ RNA levels
E
N3 T3 N6 T6 N17 T17
220
40
[kDa]
PTPRJ
β-actin

Figure 2

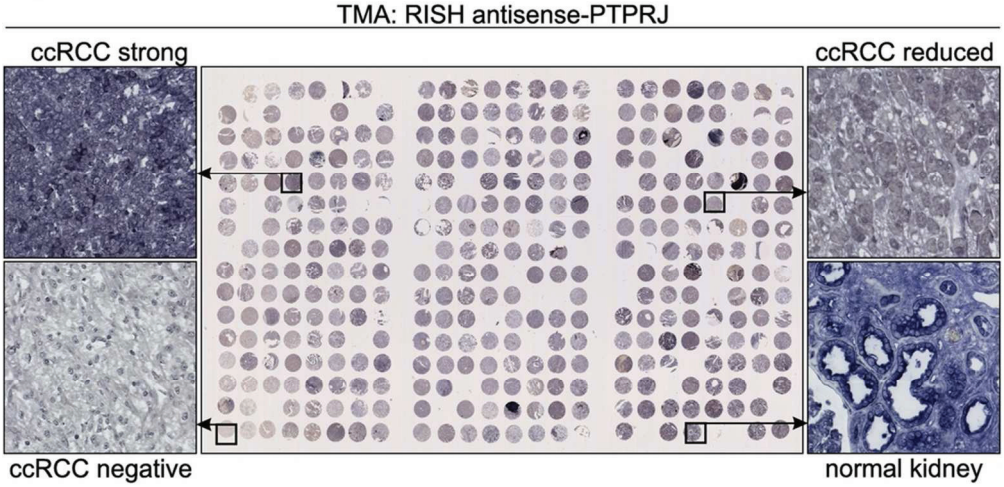
TMA: RISH antisense-PTPRJ
ccRCC strong
ccRCC reduced
ccRCC negative
normal kidney

Figure 3

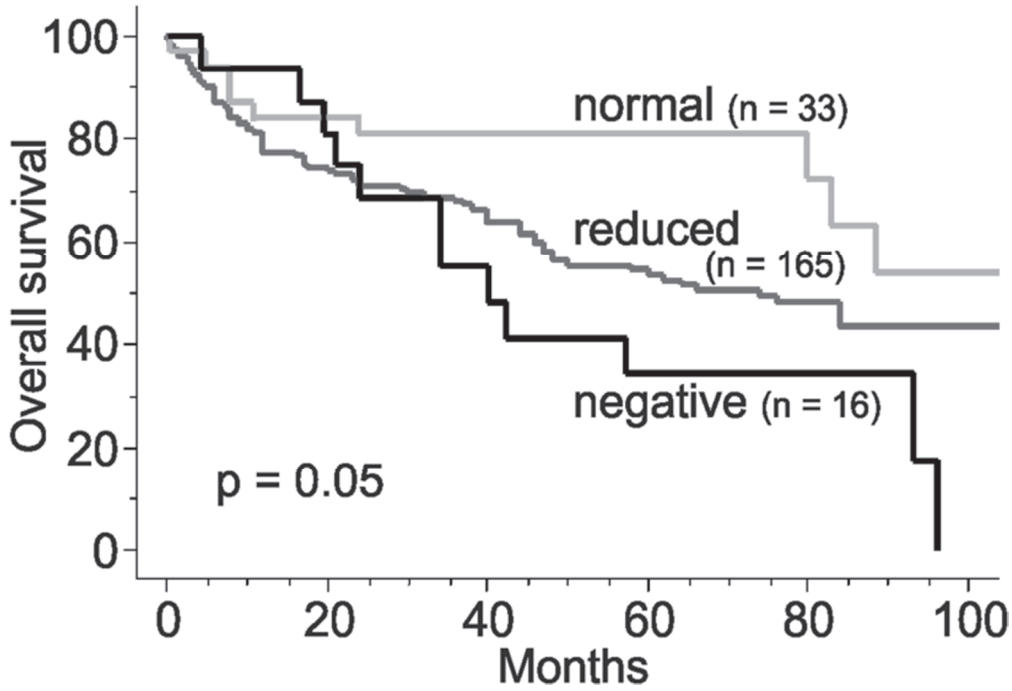
100
80
60
40
20
0
Overall survival
normal (n = 33)
reduced
(n = 165)
negative (n = 16)
p = 0.05
0
20
40
60
80
100
Months

Figure 4

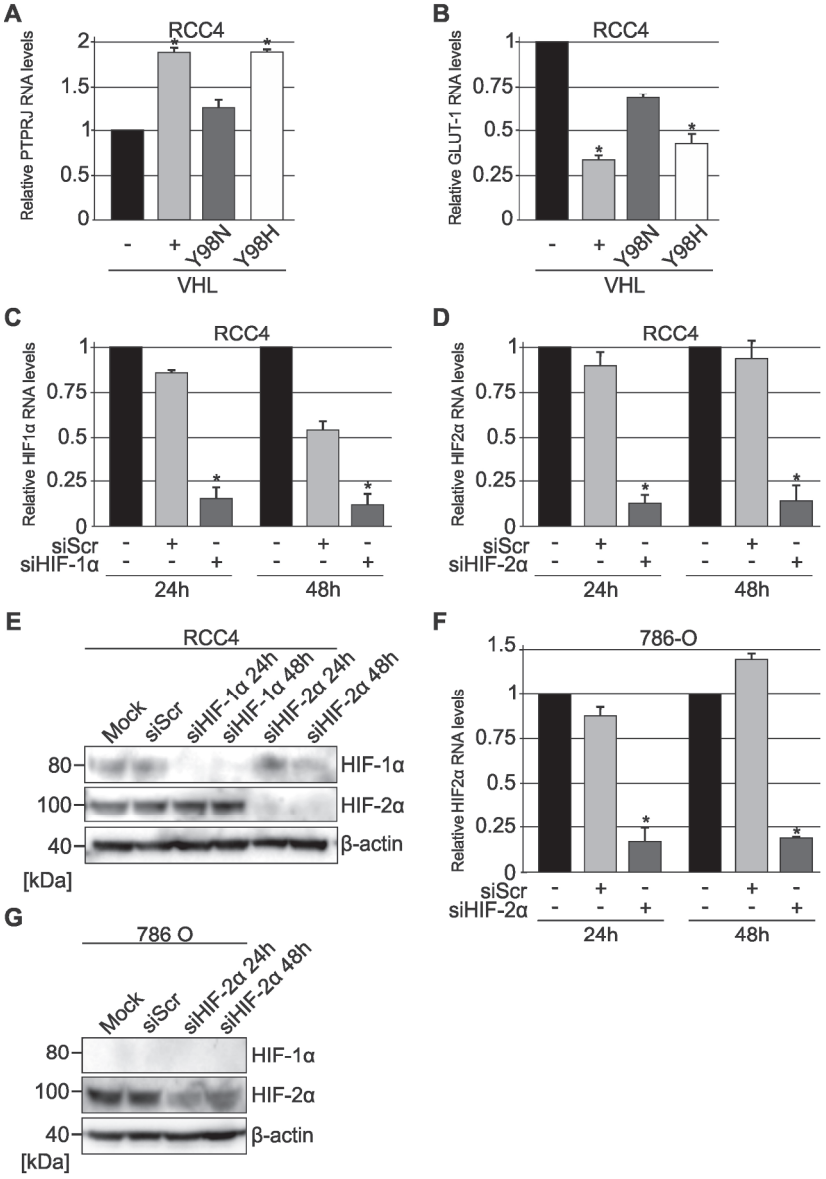
A
RCC4
Relative PTPRJ RNA levels
2
1.5
1
0.5
0
-
+
Y98N
Y98H
VHL
B
RCC4
Relative GLUT-1 RNA levels
1
0.75
0.5
0.25
0
-
+
Y98N
Y98H
VHL
C
RCC4
Relative HIF1α RNA levels
1
0.75
0.5
0.25
0
siScr
siHIF-1α
24h
48h
D
RCC4
Relative HIF2α RNA levels
1
0.75
0.5
0.25
0
siScr
siHIF-2α
24h
48h
E
RCC4
Mock
siScr
siHIF-1α 24h
siHIF-1α 48h
siHIF-2α 24h
siHIF-2α 48h
80
100
40
[kDa]
HIF-1α
HIF-2α
β-actin
F
786-O
Relative HIF2α RNA levels
1.5
1
0.75
0.5
0.25
0
siScr
siHIF-2α
24h
48h
G
786 O
Mock
siScr
siHIF-2α 24h
siHIF-2α 48h
80
100
40
[kDa]
HIF-1α
HIF-2α
β-actin

Figure 5

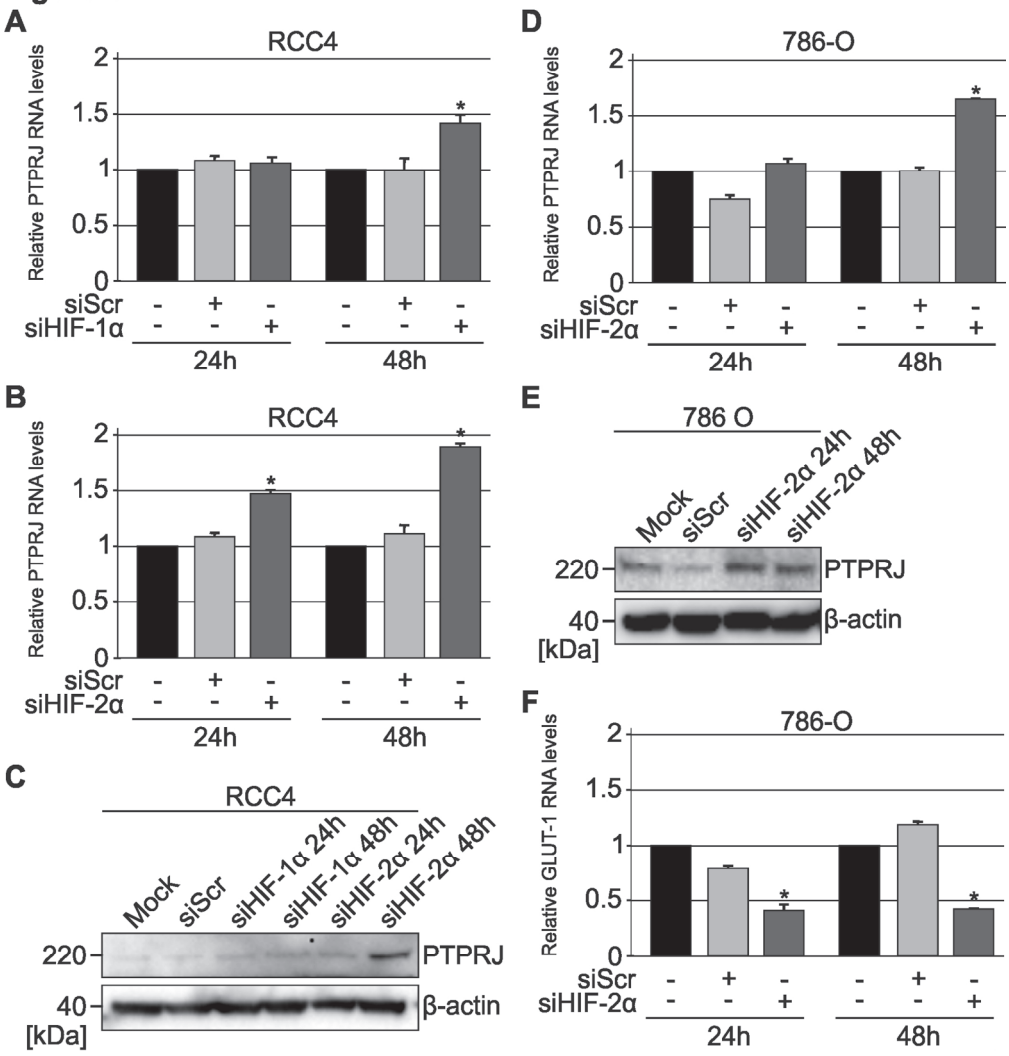
A
RCC4
Relative PTPRJ RNA levels
siScr
siHIF-1α
24h
48h
D
786-O
Relative PTPRJ RNA levels
siScr
siHIF-2α
24h
48h
B
RCC4
Relative PTPRJ RNA levels
siScr
siHIF-2α
24h
48h
E
786 O
Mock
siScr
siHIF-2α 24h
siHIF-2α 48h
220
PTPRJ
40
β-actin
[kDa]
C
RCC4
Mock
siScr
siHIF-1α 24h
siHIF-1α 48h
siHIF-2α 24h
siHIF-2α 48h
220
PTPRJ
40
β-actin
[kDa]
F
786-O
Relative GLUT-1 RNA levels
siScr
siHIF-2α
24h
48h

Figure 6

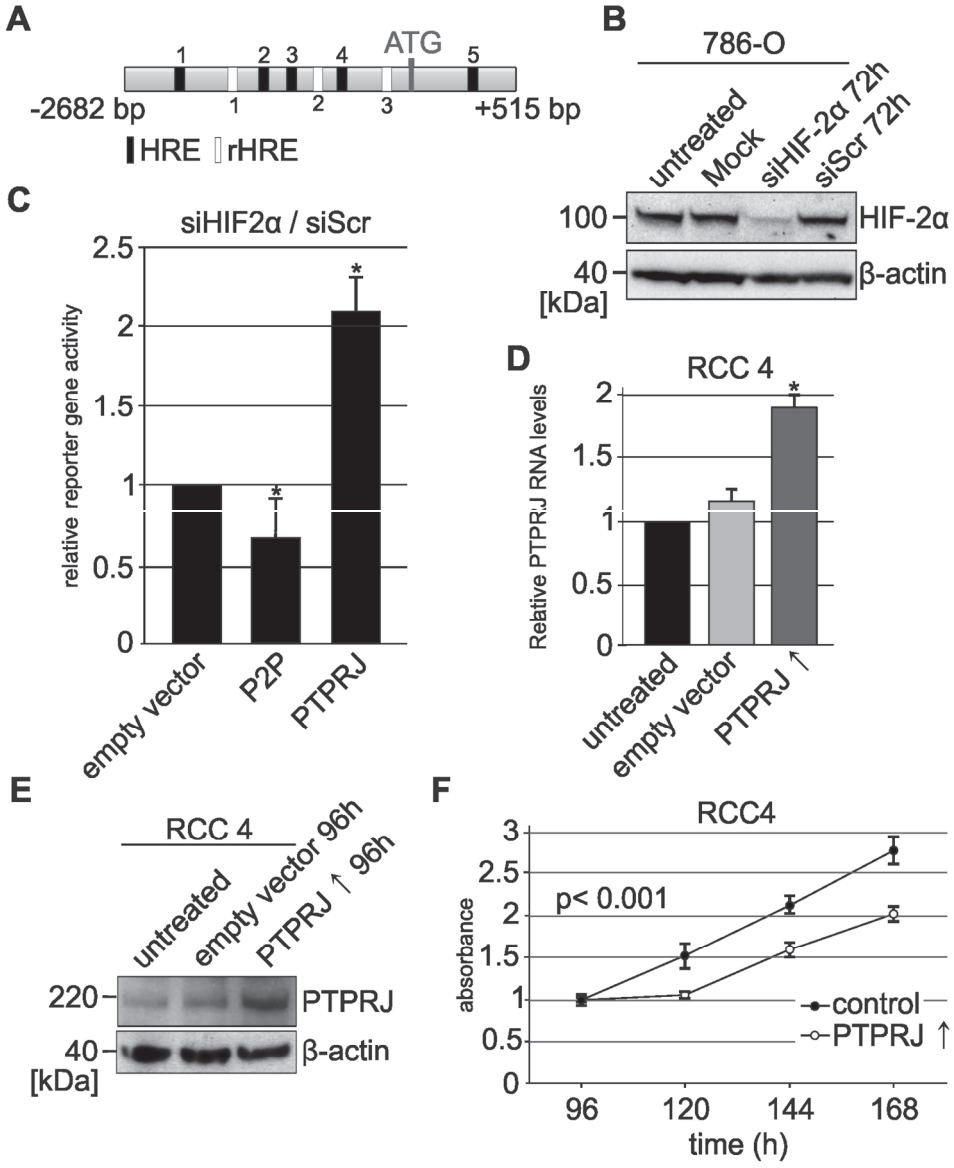
A
ATG
1
2 3
4
5
-2682 bp
1
2
3
+515 bp
HRE
rHRE
B
786-O
untreated
Mock
siHIF-2α 72h
siScr 72h
100
HIF-2α
40
β-actin
[kDa]
C
siHIF2α / siScr
relative reporter gene activity
2.5
2
1.5
1
0.5
0
empty vector
P2P
PTPRJ
D
RCC 4
Relative PTPRJ RNA levels
2
1.5
1
0.5
0
untreated
empty vector
PTPRJ ↑
E
RCC 4
untreated
empty vector 96h
PTPRJ ↑ 96h
220
PTPRJ
40
β-actin
[kDa]
F
RCC4
absorbance
p< 0.001
3
2.5
2
1.5
1
0.5
0
control
PTPRJ ↑
96
120
144
168
time (h)